Hyper Gaussian windows with fractional wavefronts

Jorge Ojeda-Castañeda,*[1] Sergio Ledesma,[1] and Cristina M. Gómez-Sarabia[2]

[1] *Electronics Department, University of Guanajuato, 36885, Salamanca, Guanajuato, México*
[2] *Digital Arts Department, University of Guanajuato, 36885, Salamanca, Guanajuato, México*

Received March 9, 2013; accepted 27, 2013; published March 31, 2013

Abstract— For reducing the impact of focus errors on the modulation transfer function (MTF), we explore the use of fractional phase power masks combined with either sub Gaussian windows, or super Gaussian windows. We present a sub Gaussian mask combined, with an asymmetric fractional phase profile, which reduces both the variations of the MTF vs. focus errors and the oscillations of the MTF around its tendency curve. However, this mask also reduces the light throughput by a factor of two.

There is a research trend aiming to extend the field depth of an optical system without reducing the size of the pupil aperture [1-10]. To that end, one acquires images using a spatial filter that reduces the influence of focus errors on the Modulation Transfer Function (MTF). At a second stage, the acquired image is digitally enhanced for compensating any modulation losses [11, 12].

Several phase masks reduce the sensitivity to focus errors at full pupil aperture. However, these phase masks generate MTFs that have unwanted oscillations around a tendency line. A Gaussian mask mitigates these undesirable oscillations [13]. In a generic manner, we denote as hyper Gaussian functions any extensions of the Gaussian function.

Here, we explore the use of fractional phase variations combined with hyper Gaussian amplitude transmittances for extending the depth of field. Specifically, we present the use of a sub Gaussian mask and a fractional wavefront, which reduces substantially the mean square error of the MTF vs. focus errors, as well as unwanted oscillations in the generated MTF.

For the sake of clarity, we discuss 1-D pupil apertures, which can be easily extended to 2-D apertures with rectangular symmetry. In Fig. 1 we depict schematically the telecentric optical system under discussion. At the pupil aperture, the generalized pupil function is

$$Q(\mu;W) = e^{i2\pi W\left(\frac{\mu}{\Omega}\right)^2} e^{i2\pi a\,\mathrm{sgn}(\mu)\left(\frac{\mu}{\Omega}\right)^t} e^{-2\pi c\left(\frac{\mu}{\Omega}\right)^s} \mathrm{rect}\left(\frac{\mu}{2\Omega}\right). \qquad (1)$$

* E-mail: jorge_ojedacastaneda@yahoo.com

In Eq. (1) the Greek letter μ represents the spatial frequency variable, whose maximum value is the cut-off spatial frequency Ω. The upper case letter W is a shorthand notation for the values of the wavefront aberration coefficient $W_{2,0}$ measured in units of wavelength.

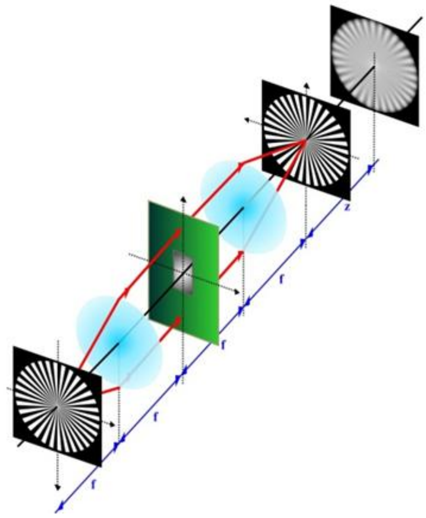

Fig. 1. Schematic diagram of the optical setup.

The lower case letter "a" is the maximum value of the optical path difference, associated with the fractional phase variation. We denote as sgn(μ) the signum function of the variable μ. The lower case letter "t" is a positive real number, which represents the fractional power of the proposed wavefront. The lower case letter "c" is the dimensionless damping factor of the hyper Gaussian functions. The lower case letter "s" is a positive real number, which represents the power of the hyper Gaussian functions. We employ the following notation. For $s < 2$ the amplitude transmittance is denoted as sub Gaussian; for $s = 2$, the amplitude transmittance is represented by a Gaussian function; while for $s > 2$, the amplitude transmittance is denoted as supergaussian. We employ the generic word hyper Gaussian for encompassing the cases $0 < s < 10$.

For variable values of focus error, the normalized irradiance distribution of the impulse response is

$$|q(x;W)|^2 = \left| \int_{-\infty}^{\infty} Q(\mu;W)\, e^{i2\pi x\mu}\, d\mu \right|^2 . \quad (2)$$

And of course, the MTF is

$$|H(\mu;W)| = \left| \int_{-\infty}^{\infty} |q(x;W)|^2\, e^{-i2\pi x\mu}\, dx \right| . \quad (3)$$

We evaluate numerically Eqs. (2) and (3) for several values of the parameters in Eq.(1). For this task, we employ the fast Fourier transform (FFT) algorithm that is described in reference [14]. Our numerical simulations use 1024 points and they include a set of Graphic User Interface (GUI) elements. The whole numerical process is written in C++ language using the Standard Template Library (STL). We start our numerical search by considering wavefronts with fractional order around t = 2.8. Then, we select weak absorption masks that are described by a dimensionless damping factor c = 0.25. Next, we explore the influence of the hyper Gaussian profiles (value of s) on the MTF. For fine tuning our search, we evaluate numerically the mean square error of the MTF. The values of the optical path difference (parameter a) are changed until we obtain a MTF that has reduced mean square error.

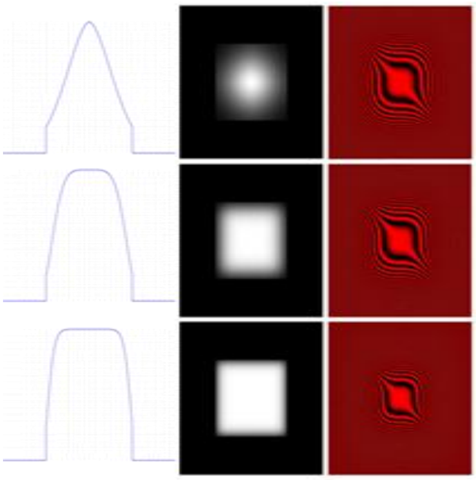

Fig. 2. Amplitude transmittance profiles, 2-D gray level pictures, and 2-D interferograms.

In Fig. 2, we illustrate our numerical results. Along column 1, we show the 1-D amplitude transmittance profiles of the selected hyper Gaussian masks. Along column 2, we display the 2-D gray level pictures of the amplitude masks. And along column 3, we show the 2-D interferograms associated with companion fractional power wave fronts.

We note that along the first line of Fig. 2, we have a weakly attenuating sub Gaussian window whose damping factor is c = 0.256. In this case, the power of the Gaussian like function is s = 1.75. And as the optical path difference, we set a = 27. The power of the fractional wavefront is t = 2.75. Now, along the second line of Fig. 2, we set c = 0.26 for a super Gaussian window, with s = 5. For the second case, the optical path difference is a = 30.864, and the power of the fractional wavefront is t = 2.758. Finally, along the third line of Figure 2, we evaluate numerically the case c = 0.212 for a super Gaussian window, with s = 10. In this latter case, we set a = 53.858, and the power of the fractional wavefront is t = 2.852. It is apparent from Fig. 2 that for the three cases, here discussed, the parameters of the attenuation windows, as well as the parameters of the phase masks have feasible optical characteristics.

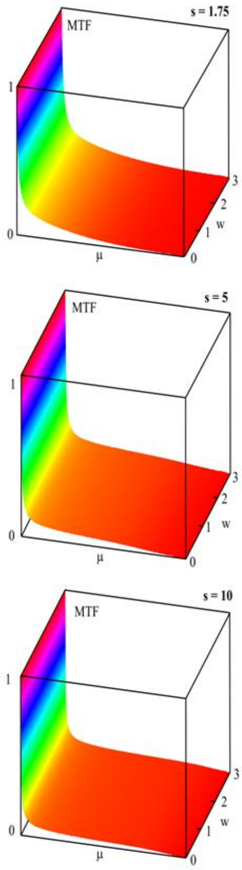

Fig. 3. Modulation Transfer Function (MTF) with variable focus error.

In Fig. 3 we show three graphs that display the MTF that is generated by employing the three optical masks in Fig. 2. From the graphs depicted in Fig. 3, we recognize that in the three cases the MTF's have low sensitivity to focus error, for the range $0 \le W \le 3$. For a given spatial frequency, as we increases the focus error the variations of the MTF have a mean square error which is less than 10^{-4}.

From Fig. 3, one can also recognize that the MTF's have a monotonic decreasing trend, which does not have zero crossings in the passband. Furthermore, the values of the MTF's do not show spurious oscillations.

However, we note that the values of the MTF and the width of the central peak tend to reduce their values as one increases the power of the hyper Gaussian window. In Fig. 4, we show the numerical evaluations of the rate of change of the MTF vs. spatial frequency. From Fig. 4, we recognize that the derivative of the MTF increases as we increase the power of the hyper Gaussian window. However, the position of the inflection point does not change with the value of s.

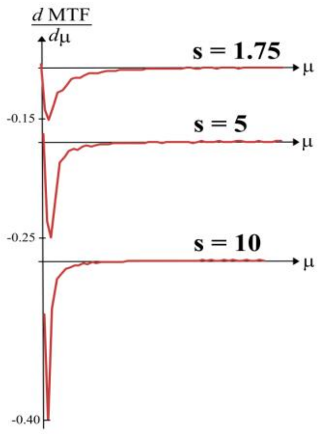

Fig. 4. Rate of change of the MTF for three hyper Gaussian masks.

Therefore, for reducing the rate of change of the MTF we recommend the use of the sub Gaussian mask with a damping factor c = 0.256, and with a fractional phase wavefront with power s = 1.75. It is relevant here to comment on influence of the proposed masks on the light gathering power of an optical system. The normalized version of the light throughput is

$$T = \frac{1}{2\Omega} \int_{-\infty}^{\infty} \left| Q(\mu; W) \right|^2 \, d\mu. \quad (4)$$

We evaluate numerically the values of T for the above discussed masks. For the mask in line one in Figure 2, the normalized light throughput is T = 0.445. For the other masks, along lines 2 and 3 in Figure 2, the values are T = 0.723 and T = 0.858, respectively. Hence, the benefits obtained by using the sub Gaussian masks come with a reduction of the light gathering power, by a factor slightly higher than two, which is equivalently to an increment in two values of F/number. However, we emphasize that by using the proposed mask one preserves the resolution associated with a full aperture, and an extended depth of the field.

Summarizing, for reducing the influence of a focus error on the MTF, we have suggested employing simultaneously weak attenuation amplitude masks and fractional power wavefronts. For describing the attenuation masks, we have used exponential decreasing functions whose argument is a monomial to the "s" power. Clearly, for s = 2, one has an amplitude transmittance that is proportional to a Gaussian function. The amplitude transmittance is represented by sub Gaussian functions, if s < 2. And for s > 2, one has amplitude transmittances represented by super Gaussian functions. From our numerical simulations we have identified three combinations of weak attenuation masks and fractional power wavefronts which are able to generate MTF´s with low sensitivity to a focus error, within the range $0 \leq W \leq 3$. Specifically, we have unveiled a sub Gaussian window, of order s = 1.75, and with a fractional wavefront of order t = 2.75, which has a MTF with a slow rate of change. The proposed sub Gaussian masks preserve the resolution associated with a full aperture. However, these optical characteristics come at the expense of reducing the light gathering power by a factor slightly greater than two.

We gratefully acknowledge the financial support of CONACYT (157276) and PROMEP (103.5/10/46.12, and PTC-197 D).

References

[1] M. Mino, Y. Okano, Appl. Opt. **10**, 2219 (1971).
[2] J. Ojeda-Castañeda, L.R. Berriel Valdos, E.L. Montes, Opt. Lett. **8**, 458 (1983).
[3] J. Ojeda-Castañeda, L.R. Berriel-Valdos, E. Montes, Appl. Opt. **27**, 790 (1988).
[4] E.R. Dowski, T.W. Cathey, Appl. Opt. **34**, 1859 (1995).
[5] N. George, W. Chi, J. Opt. A - Pure Appl. Opt. **5**, s157 (2003).
[6] A. Sauceda, J. Ojeda-Castañeda, Opt. Lett. **29**, 560 (2004).
[7] A. Castro, J. Ojeda-Castañeda, Appl. Opt. **43**, 3474 (2004).
[8] S. Mezouari, G. Muyo, A.R. Harvey, J. Opt. Soc. Am. A **23**, 1058 (2006).
[9] J. Ares García, S. Bará, M. Gomez García, Z. Jaroszewicz, A. Kolodziejczyk, K. Petelczyc, Opt. Exp. **16**, 18371 (2008).
[10] J. Ojeda-Castañeda, J.E. A. Landgrave, C.M. Gómez-Sarabia, Appl. Opt. **47**, E99 (2008).
[11] J. Ojeda-Castañeda, A. Noyola-Isgleas, Appl. Opt. **27**, 2583 (1988).
[12] W.T. Cathey, E.R. Dowski, Appl. Opt. **41**, 6080 (2002).
[13] J. Ojeda-Castañeda, E. Yépez-Vidal, E. García-Almanza, C.M. Gómez-Sarabia, Phot. Lett. Poland **4**, 115 (2012).
[14] N. Brenner and C. Rader, IEEE Acoustics, Speech Signal Proc. **24**, 264 (1976).

